0026-895X/93/020451-10$03.00/0
Copyright © by The American Society for Pharmacology and Experimental Therapeutics
All rights of reproduction in any form reserved.
MOLECULAR PHARMACOLOGY, 44:451-460

MOL PHARM

Isolation and Pharmacological Characterization of ω-Grammotoxin SIA, a Novel Peptide Inhibitor of Neuronal Voltage-Sensitive Calcium Channel Responses

RICHARD A. LAMPE, PATRICIA A. DEFEO, MATTHEW D. DAVISON, JANICE YOUNG, JOSEPH L. HERMAN, RUSSELL C. SPREEN, MICHAEL B. HORN, THOMAS J. MANGANO, and RICHARD A. KEITH

Departments of CNS Pharmacology (R.A.L., P.A.D., M.B.H., T.J.M., R.A.K.), Structural Chemistry (J.L.H., R.C.S.), and Biotechnology (M.D.D., J.Y.), Zeneca Pharmaceuticals, a Business Unit of Zeneca Inc., Wilmington, Delaware 19897, and Zeneca Pharmaceuticals, Alderley Park, Macclesfield, Cheshire, UK SK10 4TG (M.D.D., J.Y.)

Received February 5, 1993; Accepted May 18, 1993

SUMMARY

ω-Grammotoxin SIA, a peptidergic blocker of voltage-sensitive calcium channel (VSCC) responses, was purified from *Grammostola spatulata* (tarantula spider) venom by reverse phase high performance liquid chromatography. Protease-sensitive biological activity was monitored by determining the inhibition of K^+-stimulated influx of $^{45}Ca^{2+}$ into rat brain synaptosomes. Electrospray mass spectrometry indicated an average molecular mass of 4109.2 Da for the native peptide. Chemical reduction of ω-grammotoxin SIA indicated the presence of three disulfide bridges. Primary sequence data confirmed the existence of six cysteine residues and 36 residues in total, with an average theoretical molecular mass of 4109.7 Da for the amidated carboxyl-terminal species. The biological profile of ω-grammotoxin SIA indicated virtually complete blockade of presynaptic vertebrate N-type as well as P-type VSCC responses. Specifically, ω-grammotoxin SIA caused a concentration-dependent and virtually complete inhibition of K^+-evoked influx of $^{45}Ca^{2+}$ into either rat or chick brain synaptosomes. Similar inhibition profiles were generated for the inhibition of release of either D-[^{3}H]aspartate or [^{3}H]norepinephrine from rat hippocampal or [^{3}H]norepinephrine from chick cortical brain slice preparations evoked by K^+ depolarization. As reported earlier, ω-grammotoxin SIA did not inhibit ^{125}I-ω-conotoxin GVIA, [^{3}H]PN 200–110, or [^{3}H]desmethoxyverapamil binding to neuronal membrane fragments. To our knowledge, ω-grammotoxin SIA is the first ligand identified to block putative N-channel function without displacement of ^{125}I-ω-conotoxin GVIA. ω-Grammotoxin SIA thus represents a novel vertebrate VSCC antagonist that inhibits neuronal N- and P-type VSCC responses.

The classification of functionally distinct voltage-sensitive ion channels is a complicated endeavor dependent upon the discovery of novel pharmacological agents, both natural and synthetic, that uniquely interact with these sites. Within the field of mammalian neuronal VSCC, four distinct channels (T, L, N, and P) have been proposed on the basis of electrophysiological studies and pharmacological selectivity profiles, using peripheral and central neuronal populations (1–5). cDNA cloning efforts have provided structural information to support the existence of at least two of these entities (5–9). However, the existence of additional channels is strongly suspected on the basis of molecular biological studies in mammalian brain that have identified multiple mRNA species encoding VSCC (10) and on the electrophysiological recording of currents that are insensitive to the current pharmacopoeia (4). Additionally, the existence of modulatory proteins directly coupled to voltage-sensitive ion channels (11, 12) has introduced other loci with potential functional significance. Given this situation, there exists a need to discover and characterize novel ligands that interact with VSCC to assist in their functional classification.

Naturally occurring toxins represent one biological repository for the identification of new pharmacological agents and, as such, have greatly facilitated the classification and characterization of voltage-sensitive channels. For mammalian VSCC specifically, novel ligands have been isolated from the venom of the predatory fish-hunting cone snail species *Conus geographus* (13) and *Conus magus* (5, 14), from the funnel web spider species *Agelenopsis aperta* (3, 15–18), and from the black mamba species *Dendroaspis polylepis* (19). Except for FTX, the low molecular mass (200–400-Da) toxin isolated from *A. aperta* (3), the toxins are structurally rigid, highly disulfide-bridged peptides that contain six or more cysteine residues and show a

ABBREVIATIONS: VSCC, voltage-sensitive calcium channel(s); ω-CgTx GVIA, ω-conotoxin GVIA; ω-Aga-IVA, ω-agatoxin IVA; ω-Aga-IIIA, ω-agatoxin IIIA; ω-GsTx SIA, ω-grammotoxin SIA; ω-CmTx MVIIC, ω-conotoxin MVIIC; KRB, Krebs-Ringer buffer; RP, reverse phase; HPLC, high performance liquid chromatography; TFA, trifluoroacetic acid; PBS, phosphate-buffered saline; SDS, sodium dodecyl sulfate; PAGE, polyacrylamide gel electrophoresis; ES-MS, electrospray mass spectrometry; FAB-MS, fast-atom bombardment mass spectrometry; HEPES, 4-(2-hydroxyethyl)-1-piperazineethanesulfonic acid; EGTA, ethylene glycol bis(β-aminoethyl ether)-*N,N,N′,N′*-tetraacetic acid; DTT, dithiothreitol; NE, norepinephrine.

MOLECULAR PHARMACOLOGY
aspet
Downloaded from molpharm.aspetjournals.org at Thammasart University on December 3, 2012

significant degree of homologous alignment. ω-CgTx GVIA, a putative N-channel-selective antagonist, irreversibly blocks a high voltage-activated, fast-inactivating, neuronal Ca^{2+} current labeled as N-type (2). Its blockade is tissue and species specific, in that the toxin selectively interacts with neuronal versus non-neuronal VSCC and preferentially blocks the influx of Ca^{2+} into avian, amphibian, and fish versus mammalian nerve terminals (20). ω-CgTx GVIA does not appear to interact with dihydropyridine-sensitive L-channels, although it does block a noninactivating Ca^{2+} current component, as well as acting reversibly in certain preparations (21, 22). ω-Aga-IVA has been identified as a P-channel-selective ligand due to its ability to inhibit the residual, non-N/non-L, high-threshold Ca^{2+} current in cerebellar Purkinje neurons and K^+-induced influx of $^{45}Ca^{2+}$ into mammalian (i.e., rat) brain synaptosomes (15). The black mamba venom peptide calciseptine appears to be a selective cardiac L-channel inhibitor, although its selectivity within neuronal populations has not been ascertained (19). Several nonselective spider and snail venom peptides, also highly cysteine enriched, that interact with invertebrate and/or vertebrate neuronal VSCC have been reported (23–26). A recently identified member of this class is ω-CmTx MVIIC, a peptide whose structure was deduced from cDNA cloning studies of venom ducts of the fish-hunting snail *C. magus* (14). ω-CmTx MVIIC is nonselective in the sense that it inhibits the functional responses of both N- and P-type VSCC and displaces ^{125}I-ω-CgTx GVIA in binding studies.

Herein, we report the structural identification and preliminary pharmacological characterization of ω-GsTx SIA, a novel peptidergic VSCC antagonist isolated from the venom of the tarantula spider species *Grammostola spatulata*. Like the previously described venom neurotoxins this peptide contains multiple disulfide bridges, and it is intermediate in size, containing a total of 36 amino acid residues. The pharmacological analysis directly compared the effects of ω-GsTx SIA with those of the N-channel-selective antagonist ω-CgTx GVIA. ω-GsTx SIA has a unique biological profile, in that it appears to inhibit neuronal N- and P-type VSCC responses but does not inhibit mammalian vascular L-type VSCC responses, invertebrate VSCC responses, or the binding of ^{125}I-ω-CgTx GVIA to neuronal membrane fragments.

Materials and Methods

RP-HPLC. RP-HPLC was performed using Zorbax RX-C8 semi-preparative (25-cm × 9.4-mm) and analytical (25-cm × 4.6-mm) columns purchased from Rockland Technologies, Inc. (West Chester, PA) and a Vydac (Hesperia, CA) C-18 analytical (25-cm × 4.6-mm) column. Semipreparative-scale RP-HPLC was done using a 5 ml/min flow rate, whereas a 1 ml/min flow rate was used for the analytical analyses. All separations were conducted with the following mobile phase: buffer A, 0.1% TFA/H_2O; buffer B, 0.1% TFA/CH_3CN. Detection of eluting entities was monitored via UV spectroscopy at 215 nm, and fractions were collected either at 1-min intervals or manually based upon UV intensity. Initial injections of 30–50 μl of crude venom were made. Consequently, multiple fractionations were carried out at each stage of the purification, with pooling of individual identical fractions. All fractions were lyophilized before resuspension in HPLC-grade H_2O for bioassay and storage at 4°. Resuspension volumes were based upon original crude venom volumes. No detectable loss of activity was seen with storage or with adherence to either plastic or glass.

UV spectroscopy. A complete UV spectrum was obtained for ω-GsTx SIA by using a 8452A diode array spectrophotometer (Hewlett Packard, Avondale, PA). Concentration of the final peptide was calculated using the λ_{max} (280 nm) for tryptophan and was found to be in good agreement with that deduced from amino acid analysis.

Cysteinyl reduction, pyridylethylation, and tryptic digestion. ω-GsTx SIA was pyridylethylated using standard protocols. Briefly, 40–50 μg of peptide were resuspended in 100 ml of a solution containing 6 M guanidine HCl, 10 mM EDTA, and 50 mM Tris, pH 8.0. The tube was flushed with nitrogen, and DTT was added to a final concentration of 60 mM before incubation at 50° for 90 min. After reduction, 1.6 μl of 4-vinylpyridine were added to the reaction and the sample was incubated for an additional 60 min at 50°. The pyridylethylated toxin sample was desalted by RP-HPLC, using a Zorbax RX-C8 analytical column, before SDS-PAGE or tryptic digestion. For generation of peptidergic fragments, pyridylethylated toxin (20 nmol/80 μg) was incubated for 20 hr at 37° in 100 mM Tris buffer, pH 8.5, containing 25 mM $CaCl_2$ and 1 μg of trypsin. The reaction volume for tryptic digestion was 200 μl. Individual fragments were separated by RP-HPLC (Zorbax RX-C8 analytical column) using a gradient of 0–60% buffer B over 60 min. Specific fragments were identified using FAB-MS and the carboxyl-terminal fragment was subjected to amino acid analysis and automated Edman sequence analysis.

Amino acid analysis. Amino acid composition analyses were performed using an Applied Biosystems 420H amino acid analyzer.

Amino-terminal sequence analysis. Amino-terminal sequencing was performed with an Applied Biosystems 475 gas-phase sequencer. SDS-PAGE was performed using a 16.5% high-cross-linked Tris-Tricine gel (27), and the peptide was electroblotted to ProBlott (Applied Biosystems) essentially as described by Matsudaira (28). Electroblotted bands were pyridylethylated in the gas phase as described previously (29). Covalent attachment of peptides via activation of carboxyl groups and reaction with arylamine-derivatized polyvinylidene fluoride using Sequalon membranes (Millipore) was performed according to the manufacturer's instructions. Alignment of the primary amino acid sequence of ω-GsTx SIA with that of ω-CgTx GVIA, ω-CmTx MVIIC, and ω-Aga-IVA was done on the basis of cysteine placement, using the adjacent cysteine residues as the common denominator.

ES-MS and FAB-MS. ES-MS spectra were acquired using a VG/Fisons QUATTRO mass spectrometer in the multichannel analysis mode. The $(M+3H)^{3+}$, $(M+4H)^{4+}$, and $(M+5H)^{5+}$ charge states were observed for each sample and mathematically transformed to yield the zero-charge state spectrum shown. Lyophilzed ω-GsTx SIA was reduced in 0.5 M DTT/0.1 M *N*-ethylmorphylene, pH 8.5, at 38° for 10 min. Flow injections containing approximately 200–400 pmol of either reduced or oxidized peptide were measured. FAB-MS was performed on a VG 70-VSE magnetic sector mass spectrometer at 1000 resolution. The distribution of positive ions sputtered from a sample/matrix-coated stainless steel surface was measured using 8-kV xenon atoms. The matrix consisted of 3:1 dithiothreitol/dithioerythritol (magic bullet).

K^+-stimulated $^{45}Ca^{2+}$ influx into rat and chick synaptosomes (P2 pellets). Synaptosomes (P2 pellets) were prepared from either rat or chick brain, minus cerebellum and brainstem, basically as described by Reynolds *et al.* (30). Tissue was homogenized in 9 volumes of 0.32 M sucrose using a loose-fitting motor-driven Teflon-glass homogenizer. The supernatant from a 1000 × *g* centrifugation (10 min) was diluted 1/1 with KRB containing choline chloride substituted for NaCl (composition, in mM): choline chloride, 140; KCl, 5; $MgCl_2$, 1.3; glucose, 10; Na-HEPES, 10; pH 7.45; aerated with O_2 for 60 min before centrifugation at 10,000 × *g* for 15 min. Resuspension of the pellet was performed in 3 ml of KRB/g wet weight of tissue (approximately 5 mg of protein/ml) with gentle homogenization (five strokes). Synaptosomes (50 μl/tube; approximately 250 μg of protein) were kept on ice for 30 min, during which time the fractionation samples were pre-equilibrated with the tissue. During the purification, all individual fractions were resuspended in H_2O to a volume equivalent to 4 times the original volume of crude venom and were then analyzed at a final crude venom equivalent dilution of 1/1000. KRB was used for the final 250-fold dilution. $^{45}Ca^{2+}$ influx was initiated by the addition of 450 μl

MOL PHARM
MOLECULAR PHARMACOLOGY
aspet
Downloaded from molpharm.aspetjournals.org at Thammasart University on December 3, 2012

of either low (5 mM) or high (50 mM; iso-osmotic substitution with choline chloride) K^+-containing KRB spiked with approximately 2 mCi/ml $^{45}Ca^{2+}$/1 mM $CaCl_2$. Rapid quenching of the influx, after a 1-sec incubation period, was accomplished by adding 3 ml of KRB that contained 10 mM Na-EGTA iso-osmotically substituted for choline chloride. Samples were immediately filtered through Whatman GF/C glass fiber filters using a Hoefer FH225V filtration instrument. Filters were washed with 3 × 4 ml of wash KRB (composition, in mM: choline chloride, 139; KCl, 5; $MgCl_2$, 1.3; $LaCl_3$, 2; glucose, 10; Na-HEPES, 10; pH 7.45) and dried at 24° for 16 hr, and the retained radioactivity was determined by liquid scintillation counting. Net voltage-dependent $^{45}Ca^{2+}$ uptake was determined as the difference between uptake in the high K^+ and low K^+ KRB buffers.

Protease treatment/sensitivity. Purified ω-GsTx SIA (approximately 13 μg; final concentration in assay, approximately 800 nM) was proteolytically digested in PBS using 240 μg (1.2 units) of crude *Streptomyces* extract (Sigma type XIV, "purified"). Control samples contained either ω-GsTx SIA in PBS without protease or PBS with protease but no ω-GsTx SIA. All samples were incubated at 37° for 1 hr and then boiled for 10 min (to inactivate proteases) before drying in a speed vacuum concentrator. Samples were subsequently reconstituted in KRB and analyzed at an original crude venom equivalent dilution of 1/1000 (i.e., 800 nM) for inhibition of K^+-stimulated influx of $^{45}Ca^{2+}$ into rat synaptosomes.

K^+-evoked neurotransmitter release from brain slices. K^+-evoked release of D-[^{3}H]aspartate and [^{3}H]NE from rat hippocampal brain slices and K^+-evoked release of [^{3}H]NE from chick cortical brain slices were performed exactly as described previously (31, 32). Brain slices were pre-equilibrated with ω-GsTx SIA for 15 min before K^+ stimulation. The concentrations of K^+ used to evoke release were as follows: 25 mM for [^{3}H]NE release from rat hippocampal slices, 50 mM for [^{3}H]NE release from chick cortical slices, and 75 mM for D-[^{3}H] aspartate release from rat hippocampal slices. As discussed previously (33), these conditions resulted in comparable control total evoked release values for each neurotransmitter.

Materials. Crude *G. spatulata* spider venom was obtained from Spider Pharm, Inc. (Feasterville, PA). D-[^{3}H]Aspartate, [^{3}H]NE, and $^{45}Ca^{2+}$ were purchased from NEN/DuPont, Inc. (Boston, MA). Sequencing-grade trypsin was supplied by Boehringer Mannheim, Inc. (Indianapolis, IN). All other chemicals were either HPLC or reagent grade.

Results

RP-HPLC isolation of ω-GsTx SIA. Initial fractionation of crude *G. spatulata* venom on the Zorbax RX-C8 semipreparative column, using a gradient of 0–60% buffer B over 60 min, is depicted in Fig. 1. The corresponding biological profile presented in Fig. 2 depicts two fractions (fractions 35 and 36) that are highly enriched for inhibition of K^+-evoked $^{45}Ca^{2+}$ influx into rat synaptosomes. Neither fraction was capable of displacing ^{125}I-ω-CgTx GVIA binding to rat hippocampal membranes (data not shown). With repetitive initial fractionations, either fraction 35 alone or fractions 35 and 36 combined were selected for further purification, depending upon the biological profile of the pooled samples. Because other arachnid and crustacean venoms are known to possess multiple VSCC-blocking entities (17, 18, 20), those fractions demonstrating moderate to low levels of activity were retained for future analyses.

Isocratic elution at 25% buffer B (i.e., CH_3CN) on the Zorbax RX-C8 column fractionated this highly enriched peak of activity into three major components and, most likely, several minor entities eluting on the shoulders of these species (Fig. 3). Peak collection at this stage was performed manually based upon the 215-nm UV signal, with peak shaving of the major absorbing components. Selective enrichment of biological activity was seen for the primary peak eluting at 13–15 min. Using a shallow gradient of 24–32% buffer B over 32 min on the Zorbax RX-C8 column (Fig. 4A), a highly purified entity was manually collected, with peak shaving of the shoulders. This purified peak, henceforth referred to as ω-GsTx SIA, was chromatographed on a C-18 RP Vydac column to monitor purity (Fig. 4B) and was used for all subsequent structural and biological analyses. Protease treatment of the purified ω-GsTx SIA sample led to a significant decrease in activity, whereas boiling for 10 min resulted in little, if any, loss of activity (Table 1). SDS-PAGE of the purified sample (data not shown) indicated the presence of a broad, intensely staining band within the 3.5–4.5-kDa range and another tighter band at approximately 7.5 kDa. Based upon this information, either the sample was not purified to homogeneity or ω-GsTx SIA is a heat-stable peptidergic species of approximately 4 kDa that contains cysteine moieties and is capable of migrating as a dimer.

Structural analyses of purified ω-GsTx SIA. The average molecular weight of ω-GsTx SIA was determined by ES-MS to be 4109.2 (Fig. 5). After thiol reduction, the average molecular weight was measured at 4115.0 (Fig. 5). Because each reduction of a disulfide bond increases the mass of a peptide by 2 Da, ω-GsTx SIA must contain three disulfide linkages, based on the 6-Da mass shift. FAB-MS confirmed a molecular weight value of 4110.4 for the protonated molecular ion of native ω-GsTx SIA (data not shown). There was no evidence for the presence of a peptidergic species at 7–9 kDa, as seen with SDS-PAGE.

Amino acid composition analysis of ω-GsTx SIA yielded the data presented in Table 2. The presence of tryptophan and cysteine, which are destroyed during hydrolysis, was inferred from UV spectroscopy and ES-MS analysis, respectively. Overestimation of the glycine content was attributed to contamination with free glycine. Using norleucine as an internal standard to correct for recovery, the crude venom concentration of ω-GsTx SIA was estimated to be 2.75 mg/ml or 670 μM. Based on the same data but using the histidine value alone to deduce concentration, a value of 3.56 mg/ml or 866 μM was obtained. Absorbance measurements at 280 nm, in conjunction with the extinction coefficient for tryprophan, indicated the crude venom concentration to be approximately 780 μM. Based upon these three values, which show good agreement, we have estimated the crude venom concentration to be 800 μM. All biological results are presented with concentration values deduced from this number.

A sample of the purified toxin (Fig. 4B) was subjected to SDS-PAGE under reducing conditions, electroblotted to ProBlott membranes, and stained with Coomassie blue. An intensely staining band of about 4 kDa was observed and, as stated previously, a fainter band at about 7.5–8.0 kDa (data not shown) was presumed to be a dimer. The 4-kDa band was subjected to amino-terminal sequence analysis and the first 30 amino acid residues were identified (see Fig. 7). The position of the cysteine residues was determined by sequencing after pyridylethylation of a duplicate blotted band. Subsequent analysis of the 8-kDa band gave the same amino-terminal sequence, confirming dimerization upon SDS-PAGE and homogeneity of the sample. The carboxyl-terminal sequence of the toxin was determined by amino-terminal sequencing of the carboxyl-terminal tryptic peptide after reduction and pyridylethylation. Five major fragments were present in the RP-

MOL PHARM
MOLECULAR PHARMACOLOGY
aspet
Downloaded from molpharm.aspetjournals.org at Thammasart University on December 3, 2012

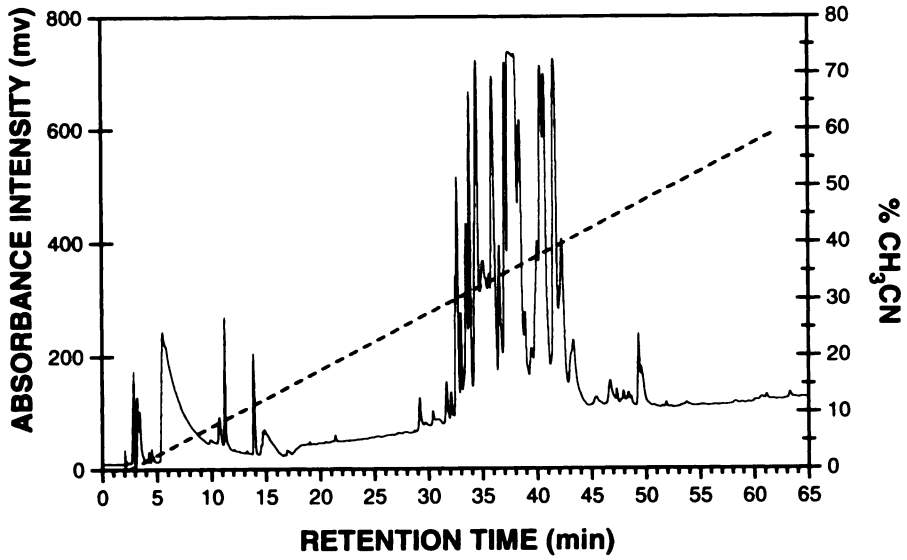

Fig. 1. Initial RP-HPLC fractionation of crude *G. spatulata* venom. Separations were performed on a Zorbax RX-C8 semipreparative column using a linear 0–60% CH_3CN gradient over 60 min, with a 3-min delay and a 5 ml/min flow rate. Injection volumes of 30–50 μl of crude venom were analyzed. Five-milliliter fractions were collected at 1-min intervals, with pooling of fractions across multiple separations. These timed pooled fractions were lyophilized before resuspension in H_2O and determination of biological activity. UV-absorbing peaks, detected at 215 nm, are expressed in mV, with 1 V being equivalent to 2.56 absorbance units. *Dashed line*, acetonitrile gradient.

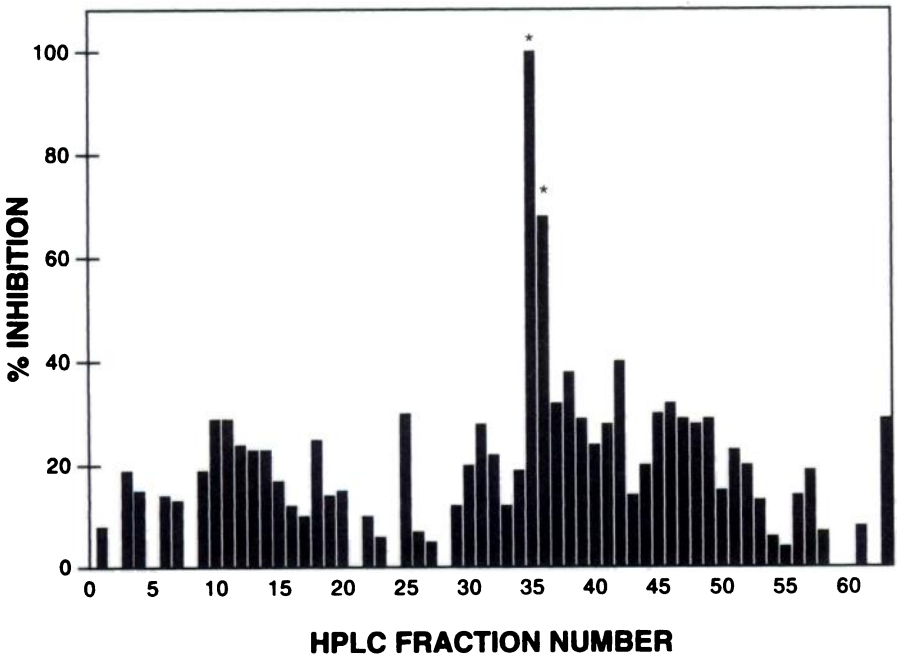

Fig. 2. Inhibition of K^+-stimulated $^{45}Ca^{2+}$ influx into rat brain synaptosomes by initial *G. spatulata* RP-HPLC fractions. Lyophilized timed (i.e., 1-min) fractions were obtained as described in Fig. 1 and were resuspended in HPLC-grade H_2O at a 1/4 original crude venom dilution. Samples were then diluted 250-fold with KRB to obtain a final assay dilution of 1/1000 original crude venom volume. Synaptosomes, prepared as described in Materials and Methods, were preincubated with each fraction for 30 min. Influx of Ca^{2+} represents the difference between the signal obtained in high (50 mM) versus low or basal (5 mM) K^+-containing KRB. Data are presented as percentage of inhibition versus control samples that contained synaptosomes in KRB without HPLC fractions. Standard error values for all data were <5%. Fractions 35 and 36 (*) were pooled for subsequent purification.

HPLC chromatogram after digestion (Fig. 6). The carboxyl-terminal fragment was identified and the sequence data determined earlier were confirmed by FAB-MS (Fig. 6). The HPLC fraction whose mass was measured as m/z 673.4 resulted from incomplete digestion of the SKWPR fragment. The structure of the carboxyl-terminal peptide, including amidation of the terminal carboxyl group, was determined as follows: a sample of the pyridylethylated carboxyl-terminal peptide was covalently attached via carboxyl groups to a Sequalon membrane and the sequence NICVWD was determined by amino-terminal sequencing. A duplicate sample was treated under conditions likely to partially deamidate a carboxyl-terminal amide, if present (i.e., exposure to gas-phase 20% aqueous TFA at 110° for 30 min), and was then sequenced after covalent attachment to a Sequalon membrane. The sequence NICVWDGSV was observed. Amino acid composition analysis of this peptide fragment indicated the expected molar ratio of the residues determined (data not shown). The expected mass of this peptidergic fragment when amidated was in total agreement with the mass value obtained from FAB-MS. Therefore, as shown in Fig. 7, ω-GsTx SIA is a 36-amino acid residue peptide containing three disulfide bonds and an amidated carboxyl terminus, with an average theoretical molecular weight of 4109.7.

Pharmacological evaluation of ω-GsTx SIA effects on neuronal VSCC responses. ω-GsTx SIA caused a concentration-dependent and nearly complete inhibition of K^+-evoked $^{45}Ca^{2+}$ influx in both chick (Fig. 8A) and rat (Fig. 8B) synaptosomes, with IC_{50} values of 270 nM and 180 nM, respectively. In contrast, ω-CgTx GVIA potently inhibited chick synaptosomal $^{45}Ca^{2+}$ influx (IC_{50} = 15 nM) (Fig. 8A) but was virtually inactive against rat synaptosomal $^{45}Ca^{2+}$ influx (IC_{50} > 10,000 nM) (Fig. 8B). Neither ω-GsTx SIA (800 nM) nor ω-CgTx GVIA (100 nM) had any effect on unstimulated $^{45}Ca^{2+}$ influx in either rat or chick synaptosomal preparations.

ω-GsTx SIA caused a concentration-dependent and nearly

MOL PHARM
MOLECULAR PHARMACOLOGY
aspet
Downloaded from molpharm.aspetjournals.org at Thammasart University on December 3, 2012

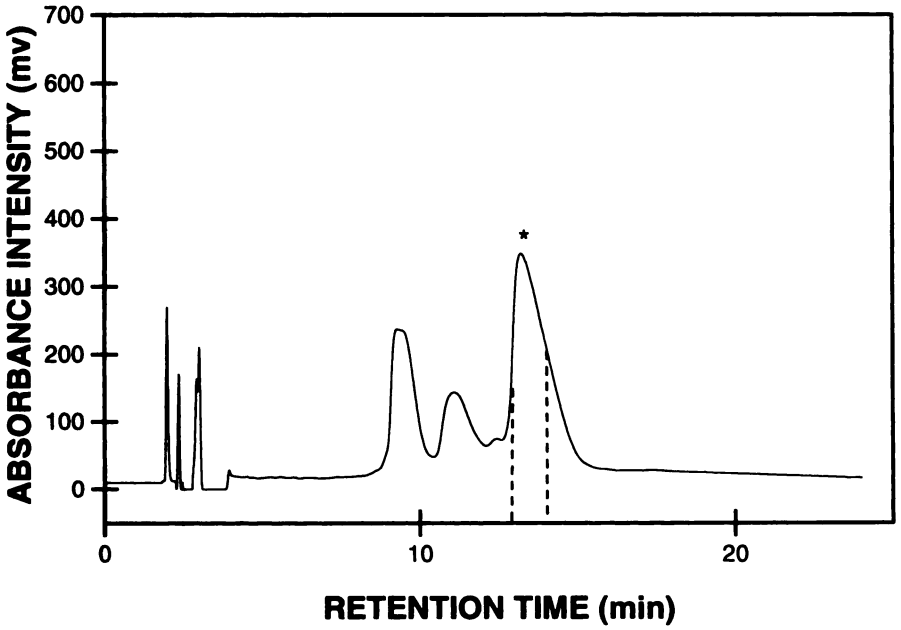

Fig. 3. Isocratic RP-HPLC separation of initially active *G. spatulata* fractions. Fractions 35 and 36 from the original chromatogram were pooled and then rechromatographed under 25% CH_3CN isocratic conditions on a Zorbax RX-C8 semipreparative column, with a 5 ml/min flow rate. Injection volumes corresponded to 50–100 μl of original crude venom. UV-absorbing peaks, detected at 215 nm, are expressed in mV, with 1 V being equivalent to 2.56 absorbance units. Discrete fractions for biological analysis were collected manually. The *dashed lines* associated with the major UV-absorbing peak depict approximately the region isolated within the biologically most active fraction (*), which was selected for further purification.

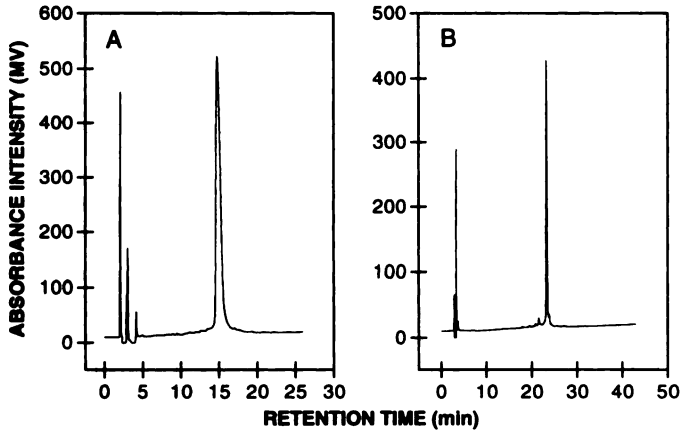

Fig. 4. RP-HPLC analysis of purified ω-GsTx SIA. A, RP-HPLC separation performed on a Zorbax RX-C8 semipreparative column using a linear 24–30% CH_3CN gradient over 24 min, with a 5 ml/min flow rate. UV-absorbing peaks, detected at 215 nm, are expressed in mV, with 1 V being equivalent to 2.56 absorbance units. B, RP-HPLC separation performed on an Vydac C-18 analytical column using a linear 20–40% CH_3CN gradient over 40 min, with a 1 ml/min flow rate. UV-absorbing peaks, detected at 215 nm, are expressed in mV, with 1 V being equivalent to 0.64 absorbance units.

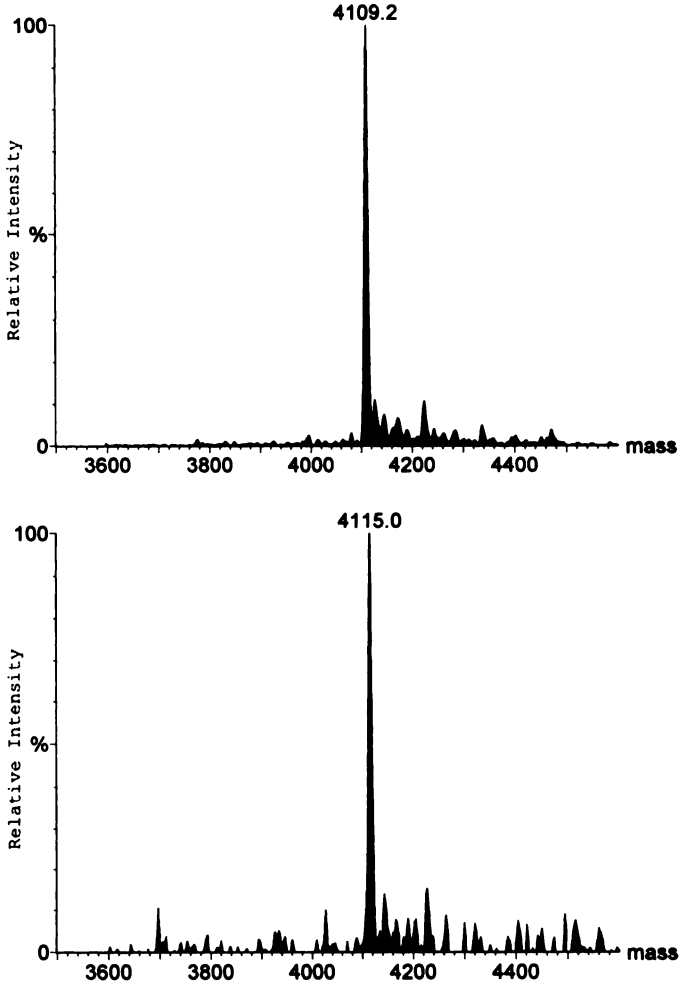

Fig. 5. ES-MS analyses of ω-GsTx SIA. *Top*, transformed ES-MS spectrum of native ω-GsTx SIA; *bottom*, DTT-reduced ω-GsTx SIA. The 6-mass unit shift in molecular weight upon reduction with DTT is consistent with the presence of three intramolecular disulfide linkages. The $3H^+$, $4H^+$, and $5H^+$ charge states were observed in each of the untransformed spectra.

TABLE 1

Protease sensitivity of ω-GsTx SIA inhibition of rat synaptosomal calcium influx

ω-GsTx SIA (800 nM) was tested against K^+-evoked rat synaptosomal $^{45}Ca^{2+}$ influx before and after protease treatment, as described in Materials and Methods. Heat treatment (95°, 10 min) was used to inactivate protease activity. Heat treatment (heat control) did not affect ω-GsTx SIA inhibition of synaptosomal flux. The values represent mean triplicate values from a single experiment that was repeated once with virtually identical results.

Condition	ω-GsTx SIA (800 nM)
	% *Inhibition*
Control	91
Heat control	88
Protease treatment	27

MOL PHARM
MOLECULAR PHARMACOLOGY
aspet
Downloaded from molpharm.aspetjournals.org at Thammasart University on December 3, 2012

TABLE 2

Amino acid composition of ω-GsTx SIA

Amino acid composition analyses were performed using an Applied Biosystems 420H amino acid analyzer. Raw data (i.e., moles/μl of venom) were normalized with respect to histidine for computation of residues/mol and comparison with Edman sequence analysis.

Residue	Total amount	Amount normalized to histidine	Edman analysis
	pmol/0.5 μl of venom	*residues/mol*	*residues/mol*
D/N	1746.5	4.0	4
E/Q	767.5	1.8	1
S	1388.0	3.2	4
G	946.0	2.1	2
H	432.0	1.0	1
R	881.0	2.0	2
T	462.0	1.1	1
A	873.0	2.0	1
P	770.0	1.8	2
Y	62.0	0.14	0
V	1129.0	2.6	3
M	16.0	ND*	0
C	186	ND*	6
I	391	0.9	1
L	544.0	1.3	1
F	388.0	0.9	1
K	1412.0	3.3	3
W	0.0	ND*	3

* Not determined due to partial or total destruction.

complete inhibition of K^+-evoked release of [^{3}H]NE from chick cortical (IC_{50} = 150 nM) (Fig. 9A) and rat hippocampal (IC_{50} = 75 nM) (Fig. 9B) brain slices, as well as the K^+-evoked release of D-[^{3}H]aspartate from rat hippocampal (IC_{50} = 210 nM) brain slices (Fig. 9C). ω-CgTx GVIA caused a potent and complete inhibition of chick brain slice [^{3}H]NE release (IC_{50} = 40 nM) (Fig. 9A) and a potent but incomplete inhibition of rat brain slice [^{3}H]NE release (IC_{50} ~ 5 nM; approximately 60% maximal inhibition) (Fig. 9B) and was inactive against rat brain D-[^{3}H] aspartate release (no effect at 3000 nM) (Fig. 9C). ω-GsTx SIA (800 nM) did not significantly displace ^{125}I-ω-CgTx GVIA, [^{3}H] PN 200–110, or D-[^{3}H]desmethoxyverapamil binding to rat brain membrane fragments and had no effect on the K^+-contracted rat aorta [Table 3; data reproduced from Keith *et al.* (34)].

Discussion

The current study describes the isolation, identification, and preliminary pharmacological evaluation of ω-GsTx SIA, a novel peptide inhibitor of neuronal VSCC responses. ω-GsTx SIA was isolated from the venom of *G. spatulata* spiders on the basis of its ability to inhibit the K^+-evoked influx of $^{45}Ca^{2+}$ into rat brain synaptosomal preparations. Similarly to previously identified peptide inhibitors of VSCC, ω-GsTx SIA is a basic peptide with multiple disulfide bridges. Specifically, ω-GsTx SIA is a 36-amino acid residue peptide of 4109.7 Da that contains three intramolecular disulfide bridges and an amidated carboxyl terminus. It is somewhat larger than the marine snail peptides ω-CgTx GVIA and ω-CmTx MVIIC but smaller than the spider peptides ω-Aga-IIIA and ω-Aga-IVA from *A. aperta*. Definitive assignment of the disulfide linkages is currently unknown but is suspected to mimic that seen for ω-CgTx GVIA.

ω-GsTx SIA presents a functional profile that is pharmacologically distinct, compared with those of other known peptide inhibitors of mammalian neuronal VSCC. Table 4 compares the effects of the snail venom peptide ω-CgTx GVIA and the *A. aperta* spider venom peptide ω-Aga-IVA with those of ω-GsTx SIA in pharmacological assays that are thought to represent biochemical measures of nerve terminal VSCC activity. ω-CgTx GVIA has been shown to cause a potent and essentially complete inhibition of chick synaptosomal $^{45}Ca^{2+}$ influx and [^{3}H]NE release from chick brain slice preparations (33, 35, 36). The relative insensitivity of these preparations to dihydropyridine L-channel antagonists (33) and ω-Aga-IVA (15, 37) suggests that these responses are mediated predominantly, if not

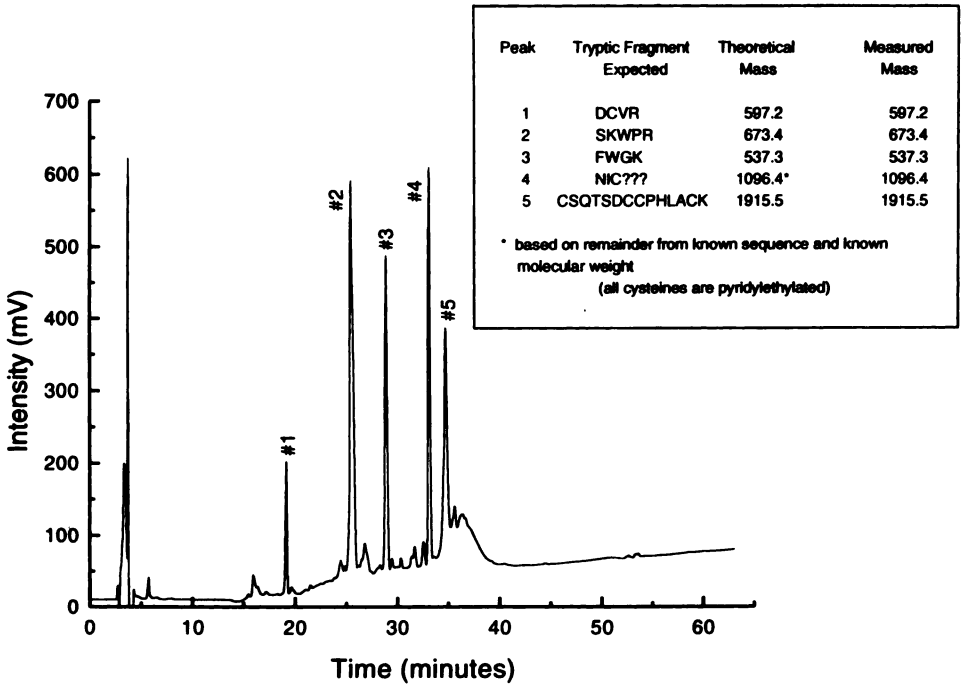

Peak	Tryptic Fragment Expected	Theoretical Mass	Measured Mass
1	DCVR	597.2	597.2
2	SKWPR	673.4	673.4
3	FWGK	537.3	537.3
4	NIC???	1096.4*	1096.4
5	CSQTSDCCPHLACK	1915.5	1915.5

* based on remainder from known sequence and known molecular weight
(all cysteines are pyridylethylated)

Fig. 6. RP-HPLC separation and FAB-MS analysis of reduced pyridylethylated ω-GsTx SIA tryptic fragments. Tryptic digestion of ω-GsTx SIA was performed on the reduced pyridylethylated toxin, as described in Materials and Methods. Individual fragments were separated on a Zorbax RX-C8 analytical column using a linear 0–60% CH_3CN gradient over 60 min, with a 1 ml/min flow rate. UV-absorbing peaks, detected at 215 nm, are expressed in mV, with 1 V being equivalent to 0.16 absorbance units. Specific fragments were identified using FAB-MS after vacuum drying of the peaks and resuspension in a 3:1 dithiothreitol/dithioerythritol matrix. Mass values correspond to the protonated molecular ion, $(M+H)^+$.

MOL PHARM
MOLECULAR PHARMACOLOGY
aspet
Downloaded from molpharm.aspetjournals.org at Thammasart University on December 3, 2012

MOL PHARM

MOLECULAR PHARMACOLOGY

SIA	D C V R F W G K C S Q T S D C C P H L A C K S K W P R N I C V W D G S V -NH2
GVIA	C K S B G S S C S B T S Y N C C R S C N B Y T K R C Y -NH2
MVIIC	C K G K G A B C R K T M Y D C C S G S C G R R G K C -NH2
Aga IVA	K K K C I A K D Y G R C K W G G T P C C R G R G C I C S I M G T N C E C K P R L I M E G L G L A -OH

Fig. 7. Primary amino acid sequence of ω-GsTx SIA. Alignment of the primary amino acid sequence of ω-GsTx SIA (*SIA*) with that of ω-CgTx GVIA (*GVIA*), ω-CmTx MVIIC (*MVIIC*), and ω-Aga-IVA was done on the basis of cysteine placement using the adjacent cysteine residues (i.e., positions 15 and 16 of ω-GsTx SIA) as the common denominator. Except for ω-Aga-IVA, all toxins contain an amidated carboxyl terminus. Within the ω-CgTx GVIA sequence, *B* designates hydroxylated proline.

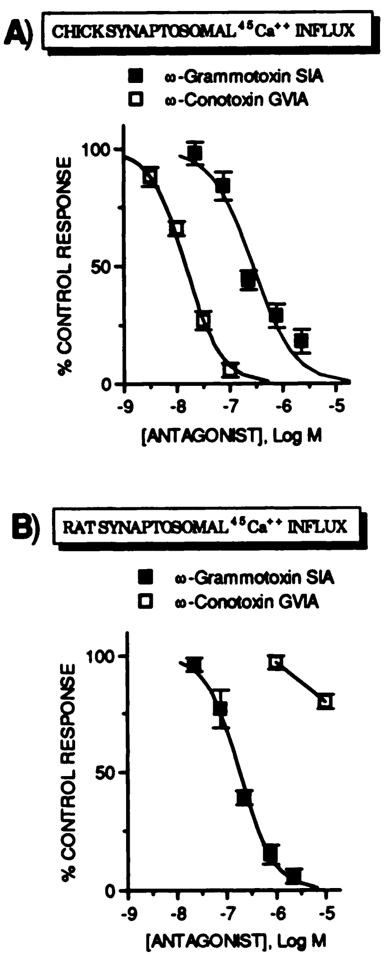

Fig. 8. Effects of ω-GsTx SIA and ω-CgTx GVIA on K^+-evoked (50 mM) chick (A) and rat (B) synaptosomal $^{45}Ca^{2+}$ influx. Data are expressed as means ± standard errors of three experiments, each performed in triplicate.

exclusively, by N-type VSCC. The observation that ω-GsTx SIA caused a potent and virtually complete inhibition of these activities implies that ω-GsTx SIA inhibits N-type VSCC. The site at which ω-GsTx SIA interacts at the N-channel, however, must be distinct from the ω-CgTx GVIA binding site, because ω-GsTx SIA failed to inhibit ^{125}I-ω-CgTx GVIA binding at concentrations (800 nM) that caused nearly maximal inhibition of the functional measures of N-channel activity (Table 3).

Rat synaptosomal $^{45}Ca^{2+}$ influx (33, 36, 38) and the K^+-evoked release of excitatory amino acids from rat hippocampal brain slices (32, 39) have been shown to be resistant to inhibition by ω-CgTx GVIA and dihydropyridines. Thus, these calcium-dependent neuronal responses represent functional measures of neuronal VSCC that are distinct from L- or N-type VSCC. The demonstration that ω-Aga-IVA inhibits a major fraction of rat synaptosomal $^{45}Ca^{2+}$ influx (15) and excitatory amino release (37, 40, 41) suggests that P-type VSCC are primarily involved. Non-L/non-N/non-P-type VSCC may also play a role in these processes, because ω-Aga-IVA appears to maximally inhibit approximately 80% of rat synaptosomal $^{45}Ca^{2+}$ influx (15). Electrophysiological evidence for neuronal high-threshold VSCC distinct from the L, N, and P subtypes supports this possibility (4). At a concentration of 2.4 μM, ω-GsTx SIA caused a 94 ± 3% inhibition of K^+-evoked rat synaptosomal $^{45}Ca^{2+}$ influx. This virtually complete inhibition of rat synaptosomal $^{45}Ca^{2+}$ influx suggests that ω-GsTx SIA can inhibit the functional response of both P-type VSCC and non-L/non-N/non-P-type VSCC in this preparation.

Whole-cell patch-clamp studies in certain neuronal populations (i.e., cerebellar Purkinje and CA1 hippocampal cells) have defined an ω-CgTx GVIA- and dihydropyridine-resistant current that exhibits a pharmacological profile similar to that seen for rat synaptosomal $^{45}Ca^{2+}$ influx. In such studies ω-Aga-IVA and ω-CmTx MVIIC have been shown to inhibit this current (14, 15). Our preliminary electrophysiological examination of ω-GsTx SIA demonstrated that 800 nM ω-GsTx SIA inhibited whole-cell voltage-gated calcium current in guinea pig hippocampal CA1 neurons more than the combined inhibitory effects of 10 μM ω-CgTx GVIA and 10 μM nifedipine (34). Although these observations suggest that ω-GsTx SIA can inhibit the resistant electrophysiological current, a thorough whole-cell patch-clamp study would be required to determine this unequivocally.

Whether the evoked release of excitatory amino acids is mediated exclusively by P-type VSCC is unclear, because in most cases sufficiently high concentrations of ω-Aga-IVA have not been tested. We recently showed that ω-Aga-IVA (100 nM)

Downloaded from molpharm.aspetjournals.org at Thammasart University on December 3, 2012

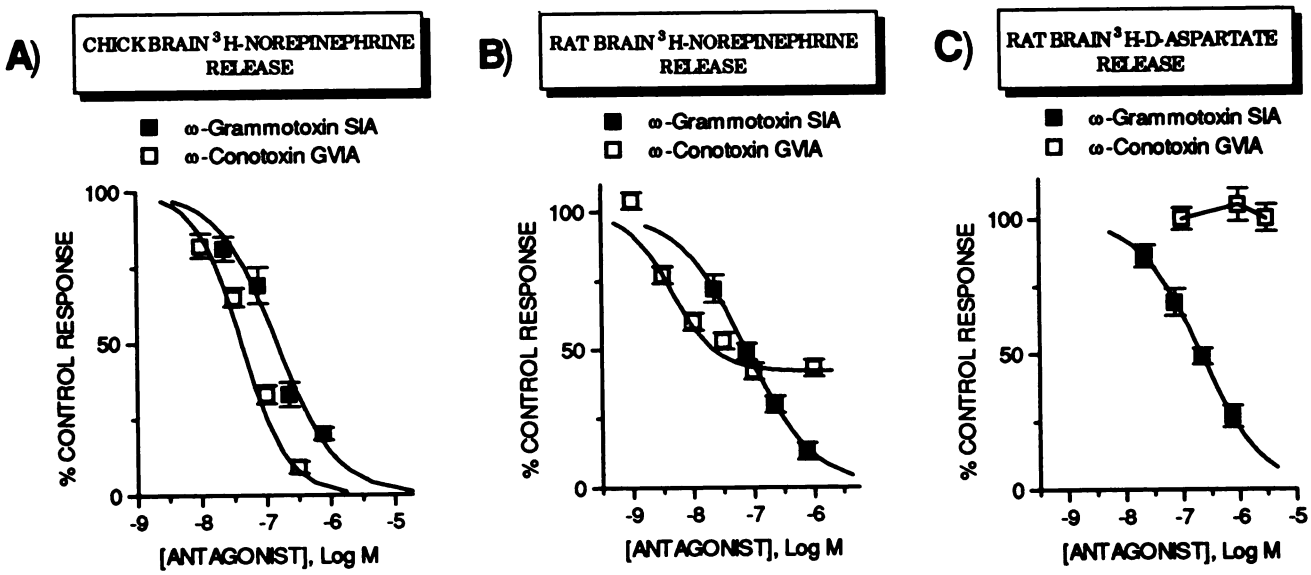

Fig. 9. Effects of ω-GsTx SIA and ω-CgTx GVIA on K^+-evoked (50 mM) release of [^{3}H]NE from chick cortical brain slices (A), K^+-evoked (25 mM) release of [^{3}H]NE from rat hippocampal brain slices (B), and K^+-evoked (75 mM) release of D-[^{3}H]aspartate from rat hippocampal brain slices (C). Data are expressed as means ± standard errors of two or three experiments, each performed in triplicate.

TABLE 3

Lack of effect of ω-GsTx SIA in selected measures of VSCC activity

ω-GsTx SIA (800 nM) was tested in binding studies and with the 80 mM K^+-contracted rat aorta as described previously (41). Values represent mean ± standard error of three experiments, each performed in triplicate, for binding studies. For rat aorta studies, two experiments were performed because of limited sample supply. (Measured parameter: relaxation.)

Assay	ω-GsTx SIA (800 nM) effect
	% of control
^{125}I-ω-CgTx GVIA binding	99 ± 4
[^{3}H]PN 200-110 binding	97 ± 3
[^{3}H]-Desmethoxyverapamil binding	94 ± 2
Rat aorta (K^+-contracted)	98

TABLE 4

Peptide toxins and VSCC responses

Effects of ω-CgTx GVIA, ω-Aga-IVA, and ω-GsTx SIA on biochemical measures of neuronal VSCC activity are shown. Flux studies refer to 50 mM K^+-evoked $^{45}Ca^{2+}$ influx in synaptosomal preparations. [^{3}H]NE release from chick cortical brain slices was evoked with 50 mM K^+ and D-[^{3}H]aspartate release from rat hippocampal brain slices was evoked with 75 mM K^+. ++, Active; NA, not active or minimally active.

	ω-CgTx GVIA	ω-Aga-IVA	ω-GsTx SIA
Chick $^{45}Ca^{2+}$ flux	++[a]	NA[b]	++
Chick [^{3}H]NE release	++[c]	NA[d]	++
Rat $^{45}Ca^{2+}$ flux	NA[e]	++[b]	++
Rat D-[^{3}H]aspartate release	NA[f]	++[d]	++

[a] From Refs. 33, 35, 36.
[b] From Ref. 15; ω-Aga-IVA IC_{50} is ~30 nM in rat synaptosomes, with 20% inhibition at 500 nM in chick synaptosomes.
[c] From Ref. 33.
[d] From Ref. 37.
[e] From Refs. 33, 35, 36, 38.
[f] From Ref. 32.

inhibited K^+-evoked release of D-[^{3}H]aspartate (37) from rat hippocampal slices by approximately 60% (limited sample supply precluded testing at higher concentrations). Similarly, a separate investigation has recently shown that 200 nM ω-Aga-IVA inhibits the K^+-evoked release of endogenous glutamate from rat hippocampal brain slices by approximately 60% (41). Turner *et al.* (40) showed that ω-Aga-IVA caused an incomplete inhibition of K^+-evoked release of glutamate from rat brain synaptosomes, with the maximal extent of inhibition being dependent on the stimulus intensity. Thus, as with synaptosomal $^{45}Ca^{2+}$ influx, P-channels may only partially mediate the evoked release of excitatory amino acids. At 800 nM, ω-GsTx SIA inhibited K^+-evoked D-[^{3}H]aspartate release by 73 ± 4% (again, testing at higher concentrations was limited due to peptide supply), demonstrating that it can cause inhibition comparable to, if not greater than, that produced by ω-Aga-IVA, although it appears to be less potent in this system. Furthermore, we have proposed that the K^+-evoked release of [^{3}H]NE from rat hippocampal brain slices is mediated by L-, N-, and P-type VSCC (33, 37). K^+-evoked release of [^{3}H]NE from rat hippocampal brain slices was inhibited 87 ± 3% by 800 nM ω-GsTx SIA, a value that is comparable to the combined inhibitory effects of ω-CgTx GVIA and ω-Aga-IVA in this preparation. This observation provides further support for the notion that ω-GsTx SIA inhibits multiple neuronal VSCC.

The polyamine antibiotic neomycin has been shown to cause concentration-dependent (IC_{50} = 90–400 μM) and virtually complete inhibition of rat and chick synaptosomal $^{45}Ca^{2+}$ influx, [^{3}H]NE release from rat and chick brain slice preparations, and D-[^{3}H]aspartate release from rat hippocampal brain slices (33). On the basis of these studies, we concluded that neomycin is a relatively nonselective inhibitor of neuronal responses that are mediated by L-, N-, and non-L/non-N-type VSCC. In this regard the biological activity of ω-GsTx SIA is very similar to that of neomycin, except that ω-GsTx SIA is approximately 3 orders of magnitude more potent. Although not evaluated in all of these assays, ω-CmTx MVIIC may be similarly nonselective, because it has been shown electrophysiologically to block N- and P-type VSCC (14) and biochemically to inhibit K^+-evoked rat synaptosomal $^{45}Ca^{2+}$ influx (14) as well as K^+-evoked release of [^{3}H]NE from rat hippocampal slices (42). In contrast to ω-GsTx SIA, however, neomycin and ω-CgTx MVIIC are effective inhibitors of ^{125}I-ω-CgTx GVIA binding. To our knowledge, ω-GsTx SIA is unique in its ability to inhibit N-channel function (e.g., chick synaptosomal $^{45}Ca^{2+}$ influx and evoked release of [^{3}H]NE from chick brain slices) without displacing ^{125}I-ω-CgTx

MOL PHARM
MOLECULAR PHARMACOLOGY
aspet
Downloaded from molpharm.aspetjournals.org at Thammasart University on December 3, 2012

GVIA from neuronal membrane fragments. Additionally, binding studies have revealed that ω-Aga-IVA does not interact with the ^{125}I-ω-CmTx MVIIC site (14), suggesting that the inhibitory effects of these peptides on P-channel function are mediated by distinct binding sites. Preliminary studies have shown that ω-GsTx SIA does not inhibit either ω-^{125}I-Aga-IVA or ^{125}I-ω-CmTx MVIIC binding.[1] These preliminary observations suggest that the inhibition of rat synaptosomal VSCC elicited by these peptides results from interactions with at least three modulatory sites.

In addition to a lack of effect on ^{125}I-ω-CgTx GVIA binding, ω-GsTx SIA (800 nM) was ineffective in inhibiting the binding of the L-channel ligands [^{3}H]PN 200–110 and [^{3}H]desmethoxyverapamil to rat synaptosomal membrane fragments (34). Other functional studies demonstrated that ω-GsTx SIA (800 nM) was inactive against 1) K^+-evoked contractions of rat aorta, a model of vascular L-type VSCC activity (34), 2) invertebrate pre- and postsynaptic VSCC at the neuromuscular junction,[2] and 3) calcium-dependent, carbachol-evoked increase of phosphoinositide turnover in SY-N-SH neuroblastoma cells.[3] Thus, at this time, the actions of ω-GsTx SIA appear to be limited to mammalian and avian neuronal VSCC.

In conclusion, the peptide ω-GsTx SIA represents a novel inhibitor of neuronal VSCC that is capable of blocking neuronal N- and P-type VSCC responses. Indirect evidence suggests that ω-GsTx SIA may also inhibit neuronal non-L/non-N/non-P-type VSCC responses. Currently there is no compelling evidence from either binding or functional studies to suggest that ω-GsTx SIA inhibits either neuronal or non-neuronal L-type VSCC. Electrophysiological analyses of tail currents in primary neuronal cultures are in progress to directly address this issue. Thus, although current studies are incomplete, available information suggests that ω-GsTx has no effect on non-neuronal VSCC. The nonselective nature of ω-GsTx effects on N- and P-type VSCC responses suggests that the toxin may interact with a regulatory site that is common to these neuronal high-threshold VSCC. Studies are ongoing to address this issue. Knowledge of the effects of ω-GsTx SIA on cloned VSCC would be beneficial to this investigation.

Acknowledgments

The authors wish to acknowledge the helpful discussions and technical contributions of Dr. Mathew M. S. Lo, Adel Verticelli, Dr. Prudence Bradley, Mr. Mike McLane, and Mr. Ty Norris. The assistance of Mr. James Huffmaster with the graphical presentations is greatly appreciated.

References

1. Nowycky, M. C., A. P. Fox, and R. W. Tsien. Three types of neuronal calcium channel with different calcium agonist sensitivity. *Nature (Lond.)* **316**:440–443 (1985).
2. Tsien, R. W., D. Lipscombe, D. V. Madison, K. R. Bley, and A. P. Fox. Multiple types of neuronal calcium channels and their selective modulation. *Trends Neurosci.* **11**:431–437 (1988).
3. Llinas, R., M. Sugimori, J.-W. Lin, and B. Cherksey. Blocking and isolation of a calcium channel from neurons in mammals and cephalopods utilizing a toxin fraction (FTX) from funnel-web spider poison. *Proc. Natl. Acad. Sci. USA* **86**:1689–1698 (1989).
4. Mintz, I. M., M. E. Adams, and B. P. Bean. P-Type calcium channels in rat central and peripheral neurons. *Neuron* **9**:85–95 (1992).
5. Olivera, B. M., L. J. Cruz, V. de Santos, G. W. LeCheminant, D. Griffin, R. Zeikus, J. M. McIntosh, R. Galyean, J. Varga, and W. R. Gray. Neuronal calcium channel antagonists: discrimination between calcium channel subtypes using ω-conotoxin from *Conus magus* venom. *Biochemistry* **26**:2086–2090 (1987).
6. Williams, M. E., P. F. Brust, D. H. Feldman, S. Patthi, S. Simerson, A. Maroufi, A. F. Mccue, G. Velicelebi, S. B. Ellis, and M. M. Harpold. Structure and functional expression of an ω-conotoxin sensitive human N-type calcium channel. *Science (Washington D. C.)* **257**:389–395 (1992).
7. Mori, Y., T. Friedrich, M. S. Kim, A. Mikami, J. Nakai, P. Ruth, E. Bosse, F. Hofmann, V. Flockerzi, and T. Furuichi. Primary structure and functional expression from complementary DNA of a brain calcium channel. *Nature (Lond.)* **350**:398–402 (1991).
8. Snutch, T. P., W. J. Tomlinson, J. P. Leonard, and M. M. Gilbert. Distinct calcium channels are generated by alternative splicing and are differentially expressed in the mammalian CNS. *Neuron* **7**:45–57 (1991).
9. Hui, A., P. T. Ellinor, O. Krizanova, J.-J. Wang, R. J. Diebold, and A. Schwartz. Molecular cloning of multiple subtypes of a novel rat brain isoform of the *alpha*-1 subunit of the voltage-dependent calcium channel. *Neuron* **7**:35–44 (1991).
10. Snutch, T. P., J. P. Leonard, M. M. Gilbert, H. A. Lester, and N. Davidson. Rat brain expresses a heterogeneous family of calcium channels. *Proc. Natl. Acad. Sci. USA* **87**:3391–3395 (1990).
11. Kleuss, C., J. Hescheler, C. Ewel, W. Rosenthal, G. Schultz, and B. Wittig. Assignment of G-protein subtypes to specific receptors inducing inhibition of calcium currents. *Nature (Lond.)* **353**:43–46 (1991).
12. Taussig, R., S. Sanchez, M. Rifo, A. G. Gilman, and F. Belardetti. Inhibition of the ω-conotoxin-sensitive calcium current by distinct G-proteins. *Neuron* **8**:799–809 (1992).
13. Olivera, B. M., J. M. McIntosh, L. J. Cruz, F. A. Luque, and W. R. Gray. Purification and sequence of a presynaptic peptide toxin from *Conus geographus* venom. *Biochemistry* **23**:5087–5090 (1984).
14. Hillyard, D. R., V. D. Monje, I. M. Mintz, B. P. Bean, L. Nadasdi, J. Ramachandran, G. Miljanich, A. Azimizoonooz, J. M. McIntosh, L. J. Cruz, J. S. Imperial, and B. M. Olivera. A new conus peptide ligand for mammalian presynaptic Ca^{2+} channels. *Neuron* **9**:69–77 (1992).
15. Mintz, I. M., V. J. Venema, K. M. Swiderek, T. D. Lee, B. P. Bean, and M. E. Adams. P-Type calcium channels blocked by the spider toxin ω-Aga-IVA. *Nature (Lond.)* **355**:827–829 (1992).
16. Mintz, I. M., V. J. Venema, M. E. Adams, and B. P. Bean. Inhibition of N- and L-type Ca^{2+} channels by the spider venom toxin ω-Aga-IIIA. *Proc. Natl. Acad. Sci. USA* **88**:6628–6631 (1991).
17. Adams, M. E., V. P. Bindokas, L. Hasegawa, and V. J. Venema. ω-Agatoxins: novel calcium channel antagonists of two subtypes from funnel web spider (*Agelenopsis aperta*) venom. *J. Biol. Chem.* **265**:861–867 (1990).
18. Pocock, J. M., V. J. Venema, and M. E. Adams. ω-Agatoxins differentially block calcium channels in locust, chick and rat synaptosomes. *Neurochem. Int.* **20**:263–270 (1992).
19. de Weille, J. R., H. Schweitz, P. Maes, A. Tartar, and M. Lazdunski. Calciseptine, a peptide isolated from black mamba venom, is a specific blocker of the L-type calcium channel. *Proc. Natl. Acad. Sci. USA* **88**:2437–2440 (1991).
20. Cruz, L. J., D. S. Johnson, J. S. Imperial, D. Griffin, G. W. LeCheminant, G. P. Miljanich, and B. M. Olivera. *omega*-Conotoxins and voltage-sensitive calcium channel subtypes. *Curr. Top. Membr. Transp.* **33**:417–429 (1988).
21. Plummer, M. R., and P. Hess. Reversible uncoupling of inactivation in N-type calcium channels. *Nature (Lond.)* **351**:657–659 (1991).
22. Plummer, M. R., D. E. Logothetis, and P. Hess. Elementary properties and pharmacological sensitivities of calcium channels in mammalian peripheral neurons. *Neuron* **2**:1453–1463 (1989).
23. Olivera, B. M., W. R. Gray, R. Zeikus, J. M. McIntosh, J. Varga, J. Rivier, V. de Santos, and L. J. Cruz. Peptide neurotoxins from fish-hunting cone snails. *Science (Washington D. C.)* **230**:1338–1343 (1985).
24. Stapleton, A., D. T. Blankenship, B. L. Ackermann, T.-M. Chen, G. W. Gorder, G. D. Manley, M. G. Palfreyman, J. E. Coutant, and A. D. Cardin. Curtatoxins: neurotoxic insecticidal polypeptides isolated from the funnel-web spider *Hololena curta*. *J. Biol. Chem.* **265**:2054–2059 (1990).
25. Branton, W. D., L. Kolton, Y. N. Jan, and L. Y. Jan. Neurotoxins from *Plectreurys* spider venom are potent presynaptic blockers in *Drosophila*. *J. Neurosci.* **7**:4195–4200 (1987).
26. Leung, H.-T., W. D. Branton, H. S. Phillips, L. Jan, and L. Byerly. Spider toxins selectively block calcium currents in *Drosophila*. *Neuron* **3**:767–772 (1989).
27. Schagger, H., and G. von Jagow. Tricine-sodium dodecyl sulfate-polyacrylamide gel electrophoresis for the separation of proteins in the range from 1 to 100 kDa. *Anal. Biochem.* **166**:368–379 (1987).
28. Matsudaira, P. Sequence from picomole quantities of proteins electroblotted onto polyvinylidene difluoride membranes. *J. Biol. Chem.* **262**:10035–10038 (1987).
29. Andrews, P. C., and J. E. Dixon. A procedure for *in situ* alkylation of cystine residues on glass fiber prior to protein microsequence analysis. *Anal. Biochem.* **161**:524–528 (1987).
30. Reynolds, I. J., J. A. Wagner, S. H. Snyder, S. A. Thayer, B. M. Olivera, and R. J. Miller. Brain voltage-sensitive calcium channel subtypes differentiated by ω-conotoxin fraction GVIA. *Proc. Natl. Acad. Sci. USA* **83**:8804–8807 (1986).
31. Keith, R. A., T. J. Mangano, M. A. Pacheco, and A. I. Salama. Characterization of the effects of ω-conotoxin GVIA on the responses of voltage-sensitive calcium channels. *J. Auton. Pharmacol.* **9**:243–252 (1989).
32. Mangano, T. J., J. Patel, A. I. Salama, and R. A. Keith. Inhibition of K^+-

[1] B. M. Olivera, personal communication.
[2] W. D. Branton, personal communication.
[3] J. Patel, personal communication.

MOL PHARM
MOLECULAR PHARMACOLOGY
aspet
Downloaded from molpharm.aspetjournals.org at Thammasart University on December 3, 2012

evoked D-aspartate release and neuronal calcium influx by verapamil, diltiazem and dextromethorphan: evidence for non-L/non-N voltage-sensitive calcium channels. *Eur. J. Pharmacol.* **192**:9–17 (1991).
33. Keith, R. A., T. J. Mangano, P. A. DeFeo, M. B. Horn, and A. I. Salama. Actions of neomycin on neuronal L-, N-, and non-L/non-N-type voltage-sensitive calcium channel responses. *J. Mol. Neurosci.* **3**:147–154 (1992).
34. Keith, R. A., P. A. DeFeo, R. A. Lampe, K. T. Spence, M. M. S. Lo, and J. M. H. ffrench-Mullen. Inhibition of neuronal calcium channels by a fraction from *Grammostola spatulata* venom. *Pharmacol. Commun.* **1**:19–25 (1992).
35. Suszkiw, J. B., M. M. Murawsky, and R. C. Fortner. Heterogeneity of presynaptic calcium channels revealed by species differences in the sensitivity of synaptosomal $^{45}Ca^{2+}$ entry to ω-conotoxin. *Biochem. Biophys. Res. Commun.* **145**:1283–1286 (1987).
36. Lundy, P. M., R. Frew, T. W. Fuller, and M. G. Hamilton. Pharmacological evidence for an ω-conotoxin, dihydropyridine-insensitive neuronal Ca^{2+} channel. *Eur. J. Pharmacol.* **206**:61–68 (1991).
37. DeFeo, P. A., T. J. Mangano, M. E. Adams, and R. A. Keith. Inhibition of ω-conotoxin GVIA insensitive neurotransmitter release by ω-Aga-IVA. *Pharmacol. Commun.* **1**:273–278 (1992).
38. Suszkiw, J. B., M. M. Murawsky, and M. Shi. Further characterization of phasic calcium influx in rat cerebrocortical synaptosomes: inferences regarding calcium channel type(s) in nerve endings. *J. Neurochem.* **52**:1260–1269 (1989).
39. Meldrum, M. J., P. Glenton, and R. Dawson. ^{3}H-D-Aspartic acid release in brain slices of adult and aged Fischer 344 rats. *Neurochem. Res.* **17**:151–156 (1992).
40. Turner, T. J., M. E. Adams, and K. Dunlap. Calcium channels coupled to glutamate release identified by ω-Aga-IVA. *Science (Washington D. C.)* **258**:310–313 (1992).
41. Burke, S. P., C. P. Taylor, and M. E. Adams. The spider toxin ω-Aga-IVA inhibits amino acid neurotransmitter release from hippocampal tissue *in vitro*. *Soc. Neurosci. Abstr.* **18**:9 (1992).
42. Gaur, S., L. Nadasdi, J. Bell, J. Ramachandran, and G. Miljanich. A novel calcium channel blocking conopeptide, SNX-230 (M-VIIC), reveals multiple components of norepinephrine release. *Soc. Neurosci. Abstr.* **18**:972 (1992).

Send reprint requests to: Richard A. Keith, Department of Pharmacology (LW 222), Zeneca Pharmaceuticals Group, a Business Unit of Zeneca Inc., Wilmington, DE 19897.

MOL PHARM
MOLECULAR PHARMACOLOGY
aspet
Downloaded from molpharm.aspetjournals.org at Thammasart University on December 3, 2012